Atmospheric Environment 198 (2019) 478–488

Contents lists available at ScienceDirect

Atmospheric Environment

journal homepage: www.elsevier.com/locate/atmosenv

Comparison of simulated radioactive atmospheric releases to citizen science observations for the Fukushima nuclear accident

Carolynne Hultquist[a,*], Guido Cervone[a,b]

[a] Geoinformatics and Earth Observation Laboratory, Dept. of Geography and the Inst. for CyberScience, The Pennsylvania State University, University Park, PA, USA
[b] Research Application Laboratory, National Center for Atmospheric Research, Boulder, CO, USA

ARTICLE INFO

Keywords:
Dispersion model
Crowdsourced
Radiation
Fukushima
HYSPLIT

ABSTRACT

Citizen science data from the Safecast project were shown to provide a reliable estimation of the spatial distribution of concentrations of elevated radiation levels around Fukushima when compared to government data. A comparison is presented between the HYSPLIT Lagrangian atmospheric transport and dispersion (T&D) model and a reflected Gaussian model to both government and Safecast contributed measurements. The advantage of contributed data with respect to the government data is that they are collected over a long period of time and have a larger spatial coverage.

First, the Safecast contributed measurements are compared to aerial surveys completed by the Department of Energy (DOE) and the National Nuclear Security Administration (NNSA). Then the HYSPLIT T&D model is run to simulate the nuclear release using high resolution terrain and meteorological data. A Gaussian dispersion model is also run for comparison using meteorological data observed at the time of the accident. The results of both models and observed data are decay corrected to December 2016 in order to use a larger quantity of contributed measurements in the comparison.

The comparison of areas of elevated radiation shows that the citizen science observations align with the prediction of models representing dynamic behavior of radionuclides dispersed in the environment. This paper shows that citizen science data can be used to validate and potentially better calibrate atmospheric T&D models.

1. Introduction

In the weeks following the 11 March 2011 Tōhoku earthquake and tsunami, the Fukushima nuclear accident attracted enormous international attention, but little information was publicly available about the extent of the radioactive atmospheric and oceanic releases (Srinivasan and Rethinaraj, 2013; Figueroa, 2013; Du Bois et al., 2012; Nakamura and Kikuchi, 2011). The Japanese government was under incredible stress to manage responses to such incredible devastation from the earthquake and tsunami along with concerns over the radioactive release. The System for Prediction of Environmental Emergency Dose Information (SPEEDI), instituted by the Japanese government in preparation for a potential nuclear disaster (Misawa and Nagamori, 2008), failed to sufficiently monitor the release for timely public notification (Povinec et al., 2013b). SPEEDI includes a network of ionizing radiation detectors that are intended to provide observed levels of radiation measurements in order to model the dispersion and distribution of a radioactive release (Funabashi and Kitazawa, 2012). Yet, in the case of the March 2011 radioactive releases from the Fukushima Daiichi Nuclear Power Plant (FDNPP), the coverage of the system was limited from 24 posts to only one functional monitoring post due to damage from the earthquake and tsunami (Povinec et al., 2013b). However, other environmental measurements of elevated radiation levels could be used to fill spatio-temporal gaps in data from static government monitoring posts.

The FDNPP is located on the east coast of Japan in an earthquake and tsunami prone region (Nakamura and Kikuchi, 2011). The terrain shifts from the coastal area which is a mostly flat temperate environment to agricultural land and then densely forested areas into the mountains. The island of Honshu is characterized by a chain of

Abbreviations: HYSPLIT, Hybrid Single Particle Lagrangian Integrated Trajectory; T&D, transport and dispersion; DOE, Department of Energy; NNSA, National Nuclear Security Administration; NOAA, National Oceanic and Atmospheric Administration; SPEEDI, System for Prediction of Environmental Emergency Dose Information; SCIPUFF, Second-order Closure Integrated Puff; Bq, Becquerel; CPM, counts per minute; μSv/h, microsieverts per hour

* Corresponding author.
E-mail addresses: hultquist@psu.edu (C. Hultquist), cervone@psu.edu (G. Cervone).
URL: http://geoinf.psu.edu (C. Hultquist).

https://doi.org/10.1016/j.atmosenv.2018.10.018
Received 6 April 2018; Received in revised form 12 October 2018; Accepted 15 October 2018
Available online 22 October 2018
1352-2310/

mountains as the central backbone which effects the flow of air particles and, as a result of the flow of dispersing particles being limited, it can lead to concentrated deposition in areas. The wind direction along the coastal area varies, but most of the time during the 2011 nuclear accident, the contaminants were dispersed to the east, over the sea, thus drastically reducing the potential concentrations over land (Povinec et al., 2013a; Lyons and Colton, 2012).

At the time of the event, around two million people lived in the Fukushima prefecture and most were effected by the earthquake, tsunami, or nuclear accident. Many local communities began evacuations, but the company in charge of the reactors and the Japanese government did not immediately acknowledge that a release occurred (Nakamura and Kikuchi, 2008). Government agencies did not provide sufficient answers on the extent of the radioactive releases and, due to the technical difficulties, an estimate from SPEEDI was not released to even the Prime Minister of Japan until 23 March 2011 (Funabashi and Kitazawa, 2012). The static ionizing radiation detectors at the FDNPP did not immediately record the magnitude of the release.

Controversy surrounded the policy for the ranges of distances given as the extent of the evacuation zone around the nuclear power plant. About 85,000 people were ordered to leave the evacuation zone that was created in the aftermath and tens of thousands more left the area (Bonner et al., 2015). Some calibrated and decay corrected government measurements were made publicly available after the event, including by the U.S. Department of Energy (DOE) and National Nuclear Security Agency (NNSA) as a large-scale airborne collection of radiation levels in the Fukushima Prefecture (Lyons and Colton, 2012).

Shortly after the incident, citizen science projects began to make volunteer contributed radiation data publicly available. Safecast is project that originated from the crisis and stayed active for many years. The Safecast team maintains a contributed set of observed measurements from Geiger counters built from off-the-shelf parts and carried by volunteers (Brown et al., 2016). The Safecast citizen-led project encouraged an open data movement to measure local real-time radiation levels (Brown et al., 2017). The radiation measurements are uploaded to a collective map as individual point measurements with GPS coordinates and a time record. Safecast has proven to be a reliable source of radiation data when compared to DOE measurements (Coletti et al., 2017; Hultquist and Cervone, 2017). It is speculated that Safecast could be used to fill temporal and spatial gaps in government produced radiation data. If citizen science data are available in gaps, the distribution of Safecast could provide a check to models at places and times of limited observational input.

The atmospheric release of radioactive particles from the Fukushima accident has been simulated with dispersion models such as the Hybrid Single Particle Lagrangian Integrated Trajectory (HYSPLIT) (Chai et al., 2015) and Second-order Closure Integrated Puff (SCIPUFF) (Cervone and Franzese, 2014). The HYSPLIT model can be calibrated with observations and applied over long distances with considerations for geographically relevant background variations such as wind direction, precipitation, and elevation. A reflected Gaussian model is also used to characterize the direction of the main release over land which dispersed primarily to the northwest of the damaged nuclear power plant. A comparison of observed values with the atmospheric dispersion models from the release could provide insight into spatial variations of the release. Additional measurements from sensors over different spatial extents could be used as outside reference points to test the reliability of the models at certain times and places.

2. Background

Spatio-temporal analysis of the environment can be applied as an approach to gain situational awareness during disasters (Tomaszewski and MacEachren, 2012; Schade et al., 2013). Earth systems models and environmental data can be integrated to improve the understanding of a phenomena of interest. Environmental monitoring to produce relevant observational data is a long-standing activity that is historically performed at a large scale by governments, academics, and industry. Collection is typically performed on a standard schedule and with repeatable collection methods. The extent of monitoring is limited by expense and, therefore, the resolution of collection is only to the degree considered necessary, despite urban areas exhibiting different trends as a result of complex environmental conditions (McGrath and Scanaill, 2013).

Environmental monitoring of different phenomena occurs to various extents depending on the perceived need. Nuclear facilities have requirements to monitor radiation levels, but this effort can be limited to static sensors directly around the reactor that rely on a power supply and the sensors may be conditioned to indicate small leaks (Povinec et al., 2013b). During a disaster, monitoring can be interrupted and it can take time to get systems back online (Sugiyama et al., 2012; Funabashi and Kitazawa, 2012). Models are reliant on quality observations to accurately depict dynamic conditions and provide ground truth. Therefore, backup alternative monitoring systems should be in place in areas at risk of nuclear incidents from complex disasters. In addition, it may be possible to incorporate data collected by citizens in the area of interest.

The literature contains cases in which spatial analysis methods are used to compare models to observations. Work by Matthias et al. (2012) compares ash dispersion from simulations to remote sensing and airborne in-situ observations. They realized that neither the atmospheric dispersion models nor the observations alone could provide a comprehensive picture necessary for operational needs. An article by Korsakissok et al. (2013) compared a radioactivity dispersion model to observations around Fukushima. Results show that the model overestimated the deposition level due to the wind in the region differing from the direction of wind at the damaged nuclear power plant. They concluded that the model does not account for local-scale variability, therefore, there are issues using it to define elevated areas of radiation. Additional sources of data could be considered to improve the resolution. Research by van der Velde et al. (2017) compared citizen science data collected by volunteer observations after one day of training to data recorded by researchers and concluded that citizen science data can contribute to data collection with the potential to improve spatial and temporal coverage.

Citizen science for environmental monitoring is a growing movement that is spurred on by technologies that enable the mass collection of geolocated data. There are varied intentions behind collecting data, that are not just topic or group specific, but even specific to individual participants (Stepenuck and Green, 2015; Seymour and Haklay, 2017). Often participants collect data on phenomena of their interest such as concerns in their local environment (Conrad and Hilchey, 2011). Environmental monitoring applications often target areas that are specifically of concern to citizens; typical activities of interest include monitoring air and water quality (Ottinger, 2010; Buytaert et al., 2014). These projects stay the most active over time in areas in which there is long-term concern so that participants get invested and maintain an interest in the monitoring project (Kinchy et al., 2016). As a demonstration of the quantity of observations, spatial extent, and time frame, the DOE dataset consists of just over 107,000 measurements over a few months after the accident in the Fukushima area while the Safecast dataset has an online collection of over a 100 million downloadable measurements globally taken continuously since 2011 (Hultquist and Cervone, 2017).

Contributed citizen science datasets encourage reflection on standards in data collection (Ottinger, 2010). Government data are collected as seen fit to understand the extent and distribution of phenomena. Whereas, citizen science data are collected by populations most interested in understanding their exposure to environmental hazards in areas they inhabit and knowing if they are at risk (McCormick, 2012). Citizen science data occurs most frequently in areas of human activity so it can be used to inform populations of their exposure

(Hultquist and Cervone, 2017). Government data can be rather sparse in areas of human structures as the focus is on broad monitoring and this difference in focus produces spatial knowledge gaps in areas of interest to citizens (Kinchy et al., 2016). Citizen science can sustain long-term interest when the phenomena impacts the lives of the population. In contrast, government data are more likely to be a short-term or sparse effort unless significant changes are expected in the environment.

Each citizen science project can be different in origin, motivation, standards, objectives, and the audience reached. Citizen science projects sparked by a crisis can move rapidly from formation to collection to sharing of data. The projects set their own standards and can operate more quickly than traditional organizations which can get bogged down by bureaucracy. At the same time, these standards can be evolving while the project is being set up and there is likely not thorough documentation available when the project is initiated. Citizen contributed data needs to be evaluated, but some projects have shown to be a valid source that can estimate trends when traditional data are not available (Hultquist and Cervone, 2017).

Citizen science radiation projects originated as a result of concerns sparked by the Fukushima accident (Hemmi and Graham, 2014), but the Safecast project continues as an open data movement to collect measurements and record radiation levels globally (Brown et al., 2016). A driving motivation behind this movement is to create a standard of what is normal so that the collection will act as an early warning system in the event of a future radioactive release. Citizens recording their own measurements was not an option during previous nuclear accidents, but technological advances enabled the public to create geolocated data on environmental conditions. Citizen science is already established as "detecting environmental exposures otherwise undetected by experts due to lack of awareness, lack of sufficient methods for exposure identification, or other limitations to science," and Safecast provides a record that populations can use to be informed of their exposure to an environmental hazard that is not detectable by human senses (McCormick, 2012; Bonner et al., 2015). The Safecast project is administered by a team based in Tokyo with a diversity of expertise required to build the device, collect data, and verify measurements (Brown et al., 2016).

A major consideration is how to represent the models and data in order to integrate them as these sources often come in varying formats which makes comparison difficult. Standardizing space, time, and units may be necessary to fuse the sources in a way that produce a direct comparison of the values of interest. Models are often visualized as rasters with values stored in each grid area while observations are often made at point locations and then averaged over a raster grid. Spatial data points can be individual observations of a phenomena of interest and have many options of how to be represented. Spatial sampling methods can be used by the collector to consistently have measurements across an area of interest dependent on the properties of the observed phenomena (Tobler, 1987).

Socially produced geolocated data are typically opportunistic so the coverage is a product of the configuration of the physical environment in which the crowd is contributing data (Connors et al., 2012). Often there are many socially produced data points at the same location, which when visualized, can result in an overplotting of points. Hot-spot analysis can be used to visualize spatial data points in order to identify extreme values. A raster surface can be created from spatial data by aggregating points based within a grid at an optimal level to visualize the phenomena of interest (Hengl, 2006). The raster format can be data sparse with gaps of no data or the data can be interpolated to estimate between observations. The extent that data should be interpolated is highly dependent on how much the phenomena of interest can change over space and if it can be assumed to be linear (Diggle et al., 1998). Raster data can be both upscaled and downscaled to fit a varying grid structure with a limitation that this can cause a loss in reliability when attempting to make a direct comparison. Therefore, if there is a pre-existing raster, it is advisable to directly fit spatial data points to that common grid instead of modifying a grid with stored values unnecessarily.

3. Methods

This article presents a methodology to compare two transport and dispersion (T&D) models and two observational datasets. The comparison of atmospheric models to observations is a challenging and necessary task (Matthias et al., 2012; Hanna et al., 2002). The models are used to simulate the atmospheric radioactive release using meteorological observations taken at the time of the accident. The radiation dose rate datasets are compared to the simulated values. The main novelty is the assessment of contributed Safecast data as a potential source to validate and calibrate numerical models.

3.1. Gaussian model

A simple Gaussian reflected dispersion model, which predicts the mean concentration C_p at a location x, y, and z generated by a source located at x_s, y_s, and z_s as:

$$C_p(x, y, z, x_s, y_s, z_s) = \frac{Q g_y g_z}{2\pi U [\sigma_y^2 \sigma_z^2]^{1/2}} \tag{1}$$

with

$$g_y = \exp\left[-\frac{(y - y_s)^2}{2\sigma_y^2}\right]; \tag{2}$$

$$g_z = \exp\left[-\frac{(z - z_s)^2}{2\sigma_z^2}\right] + \exp\left[-\frac{(z + z_s)^2}{2\sigma_z^2}\right] \tag{3}$$

where Q is the mass emission rate, U is the wind speed, and $\sigma_y(x, x_s; \psi)$ and $\sigma_z(x, x_s; \psi)$ are the crosswind and vertical dispersion coefficients (i.e. the plume spreads) where ψ describes the atmospheric stability class (i.e., $\psi = A$ to $\psi = F$). The dispersion coefficients are computed from the tabulated curves of Briggs (Araya, 1999). The result of the simulation is a concentration field generated by the release along an arbitrary wind direction θ, which in this case, corresponds to 307° (clockwise from 0 pointing North). Specifics on the optimization of this model can be found in Cervone and Franzese (2011). In the simulation, the stability class ψ is set to E because it best matches the limited ground observations measured at the time of the accident in Fukushima.

This simple model has a high spatial resolution, but it is limited in capability to simulation only in one direction. Therefore, the following model is also considered that allows for directional shifts of dispersion.

3.2. HYSPLIT model

The Hybrid Single Particle Lagrangian Integrated Trajectory (HYSPLIT) is a transport, dispersion, trajectory, and deposition model of simulated particles across space and time (Draxler and Rolph, 2012). NOAA Air Resources Laboratory applies HYSPLIT radiation dispersion using "four components: particle transport by the mean wind, a turbulent transport component, scavenging and decay, and finally the computation of the air concentration (Draxler and Rolph, 2012)." Each particle can represent more than one radionuclide gas or particle and follows the mean motion of the wind field with turbulence from velocities.

For release simulations, radiation decay is considered at each time step in the Lagrangian trajectory, but not for the decay of the material before emission. For this event, it should be fitting as much of the fission product was directly released through explosions and from the controlled emissions which were highly concentrated. Although only ^{137}Cs and ^{131}I are selected for this case, there are over 200

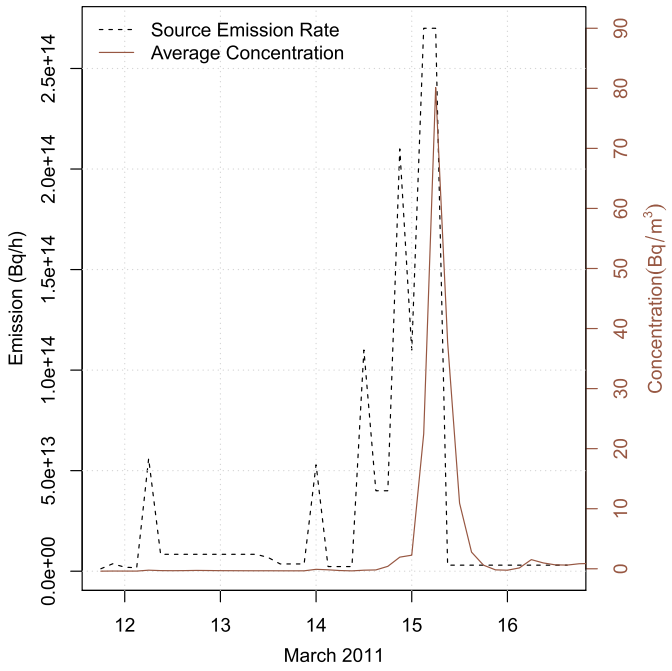

Fig. 1. Time series showing the non-steady radioactive release rate from the source used as the input of HYSPLIT (dashed) and the Average Concentration computed by HYSPLIT over the simulation domain (solid) representing the output of accumulated concentrations over land.

radionuclides built in which can be parameterized for specific radionuclides mixes. ^{137}Cs is a common nuclear reactor fission product which spreads easily, is highly water soluble, and has long term effects with a decay half-life of 30.17 years. While ^{131}I is a major concern immediately after a nuclear accident, the contribution of ^{131}I is essentially undetectable after 90 days due to its short half-life. ^{137}Cs, which does not occur naturally in the environment, is expected to be detectable for at least 600 years. ^{137}Cs is the standard radionuclide used for monitoring nuclear accidents due to its property of solely occurring in the environment as a man-made nuclear fission product. The deposition values of the model are decay corrected for comparison to the distribution of other datasets.

Due to a lack of functional sensors at the time, only estimations of the atmospheric releases from the multiple damaged reactors are available. Multiple releases are estimated using the verified source term of Terada et al. (2012) over the time of release with particles that disperse from these time periods. This source term estimation is the input for the model. The non-steady radioactive release rate used in HYSPLIT (dashed black) and the average concentration computed by HYSPLIT over the simulation domain (solid red) are shown in Fig. 1. In Fig. 1, each of these peaks in the estimation of emissions corresponds to releases at the reactor units. For the most part, the released radioactive particles dispersed towards the ocean and the high concentration of radioactive particles over land in the simulation domain is a result of a brief time of shifting winds. This release directed over land is seen on the 15th of March in Fig. 1 as the Average Concentration computed by HYSPLIT.

The transport, dispersion, and deposition calculations are run at a 3h temporal resolution at a 5 km spatial unit with vertical velocity evaluated at 50 vertical levels in relation to terrain. The Japan Meteorological Agency provided precipitation data at a 30 minute resolution for some points. As Draxler and Rolph (2012) describe, wet deposition has a significant effect that concentrates radiation particles on the surface. HYSPLIT was run using precipitation data, and therefore, wet deposition was taken into account in the output for the ground concentrations. A selection of model outputs at 3 h time steps are shown from the FDNPP (diamond symbol along coast) in Fig. 2 from 15 March 2011 at 3AM until 16 March 2011 at 3AM. During this time, the direction of dispersion changed from primarily southeast over the ocean to the northwest, depositing heavy concentrations over land. In addition, the HYSPLIT model is overlaid for visualization purposes with the DOE Extent for reference and an outline of the DOE Anomaly which is the area of elevated levels observed in the DOE data. The accumulated HYSPLIT surface is used for comparison to the other sources.

The accumulated deposition particulate ^{137}Cs Bq/m^3 is calculated with spatio-temporal consideration for wet and dry deposition. HYSPLIT is parameterized for deposition related to dry deposition velocity (set at 0.01 m/s), wet removal (Henry's constant = 3.00), non-depositing gas, and Cesium is represented with a high wet deposition rate of (0.004 m/s). As the radioactive particles are dispersed over space and time, on-ground accumulation is calculated in Becquerel which is a unit of ionizing radiation for which atoms in the material decay in a given time period.

Fig. 3 shows the accumulated concentration of radioactive particles modelled by HYSPLIT at a 5 km grid from the FDNPP to ranges of 20, 40, and 60 km away from the source. However, the observational data are not measured in Becquerel, therefore, all the units are first converted to μSv/h. Microsieverts per hour (μSv/h), from the SI unit Sievert, is a dose equivalent related to the absorbed exposure from the amount of radiation traveling through the air.

3.3. DOE data

Department of Energy (DOE)/National Nuclear Security Administration (NNSA) data was collected in the Fukushima area from 14 March 2011 to 28 May 2011 (Department of Energy, 2011; Lyons and Colton, 2012). This dataset has good spatial coverage of the Fukushima area through airborne measurements taken as swaths by following a consistent sampling pattern. The DOE Extent shown in figures is a bounded area of the maximum extent of the data collected during this period. This airborne collection provided a broad survey of the region in the weeks following the Fukushima nuclear accident. The airborne measurements in μSv/h were extrapolated to 1 m above ground level and decay corrected to 30 June 2011 before being made publicly available.

The DOE data has limited temporal coverage, but it can be extended by a method that corrects the data for decay for future dates using a longitudinal dataset as it is collected over many years and provides a point of reference (Hultquist and Cervone, 2017). The DOE data are used as a standard to compare other datasets and models by decay correcting all the data to a common date; set at the end of December 2016 for this study. The DOE Anomaly is shown in figures as an outline of the raster grid areas with average values above background radiation levels as of 30 June 2011. This area was defined through prior work that isolated areas of elevated radiation (Cervone and Hultquist, 2018).

3.4. Safecast data

Safecast provides radiation data since 2011 in areas of human activity (Hultquist and Cervone, 2017). Fig. 4 shows the quantity of Safecast data collected from 2011 to 2016 for each half-kilometer grid in the DOE identified plume of elevated radiation levels. Safecast data was analyzed in the Fukushima area in comparison to DOE data and was found to be highly correlated (Hultquist and Cervone, 2017). The first step of the methodology was a unit conversion between Safecast data, which are collected in counts per minute (CPM), to μSv/h . Temporal standardization was applied to remove the effect of background radiation and then decay correct the data to a common time in order to compare Safecast directly with DOE. The longitudinal nature of the Safecast data, as it was collected over many years, enables decay correction with an evaluation of the output to measurements taken at the time of interest. Further work refined the method to minimize error

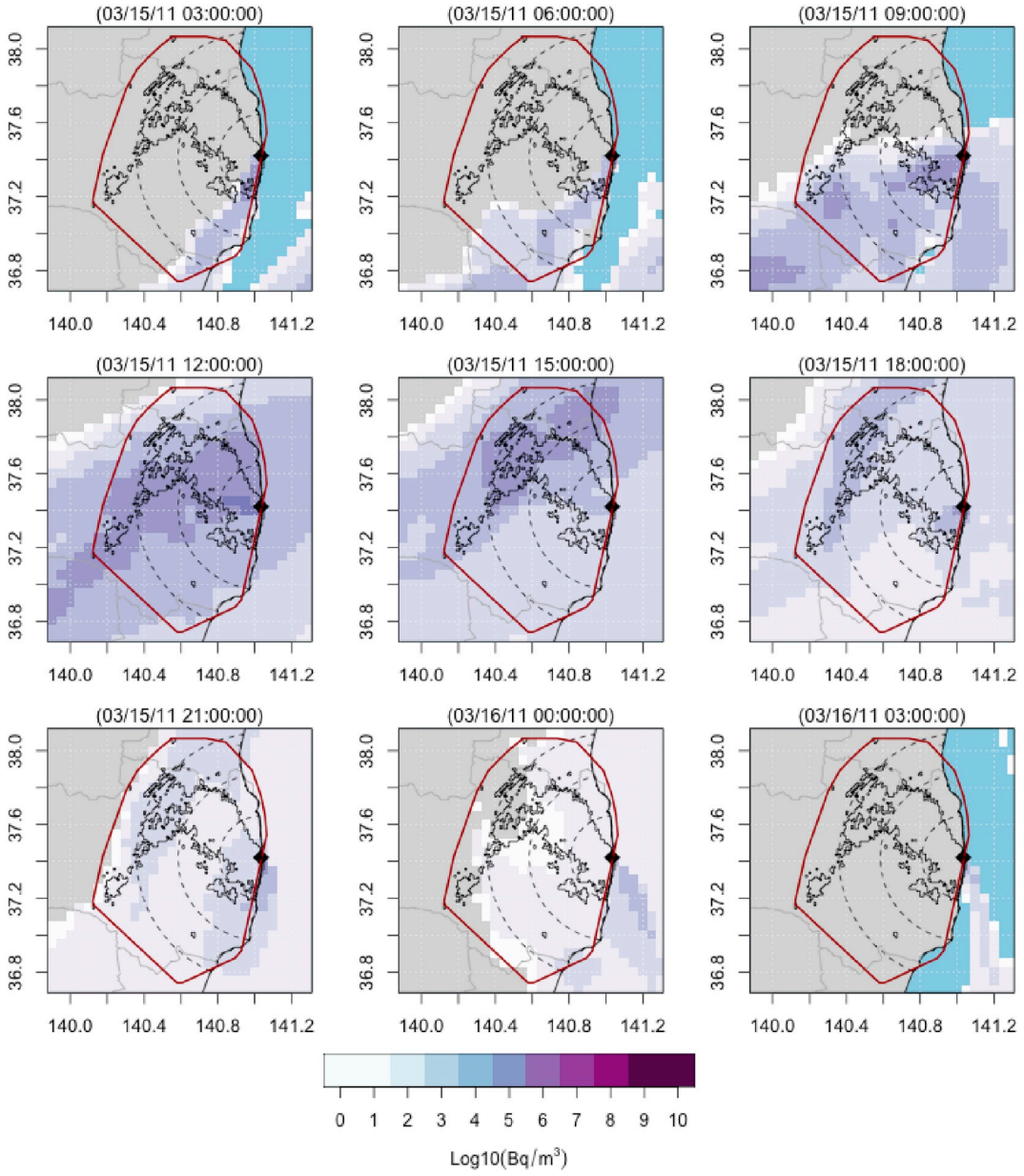

Fig. 2. The HYSPLIT model is shown at 3 h intervals on the 15th of March when radioactive particles were dispersed over land in the Fukushima area.

introduced by decay correction based on the ratio of Cesium isotopes over time and that transformation method is used to prepare the data analyzed in this paper (Cervone and Hultquist, 2018). The present article introduces a methodology for comparison of dispersion models to data within the plume in order to validate the spatial distribution of elevated levels and verify the magnitude of outputs.

4. Results

The aim of this paper is to develop a method to compare observations and models simulating the radioactive particles dispersed from the damaged FDNPP. The objective is to determine if contributed Safecast measurements could be useful to verify model results and be used as a model input if timely data are not available in sufficient quantities from other sources. This process involves unit conversion, temporal and spatial standardization, and comparison through visualization.

This article provides a methodology to compare the distribution and intensity of radiation levels from atmospheric T&D models and observations from government and contributed sources. Interpolation is avoided and scaling is only used when necessary to standardize units. This comparison builds off of previous work found in Hultquist and Cervone (2017) that developed a methodology to compare radiation datasets through spatio-temporal standardization and unit conversion. The measurements at point locations from DOE and Safecast are made into aligned half-kilometer raster grid surfaces to which the models of this study are re-sampled. The averaged value in each grid cell is used for comparison to the scaled models. Unit conversion was specified as Equation (4), the standard for the Safecast community to convert from CPM to μSv/h .

$$1\,\mu Sv/h = \frac{1}{334} CPM \tag{4}$$

An extension of the work in Cervone and Hultquist (2018) specifies transformation coefficients through the minimization of error by scaling the datasets and identifies a DOE footprint of elevated values. The current paper uses models and datasets that are spatially clipped to the extent of DOE footprint of elevated values as specified in Cervone and Hultquist (2018). The models are then scaled to the same unit. The

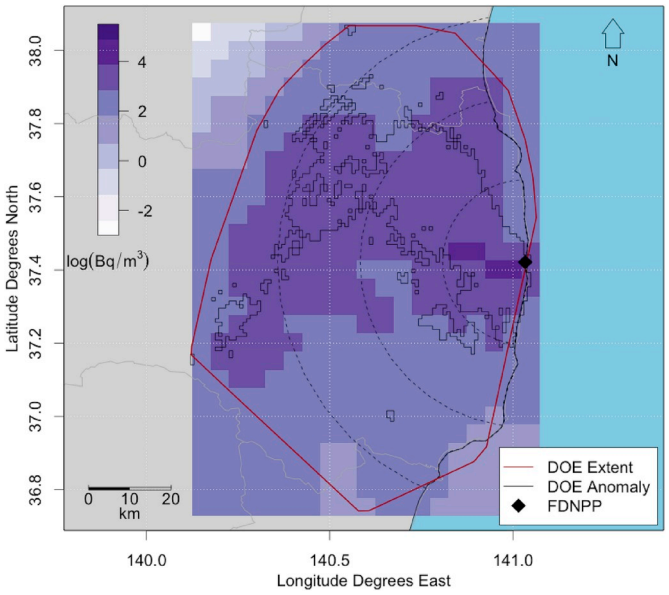

Fig. 3. Accumulated HYSPLIT plume of elevated radiation levels in Bq/m^3.

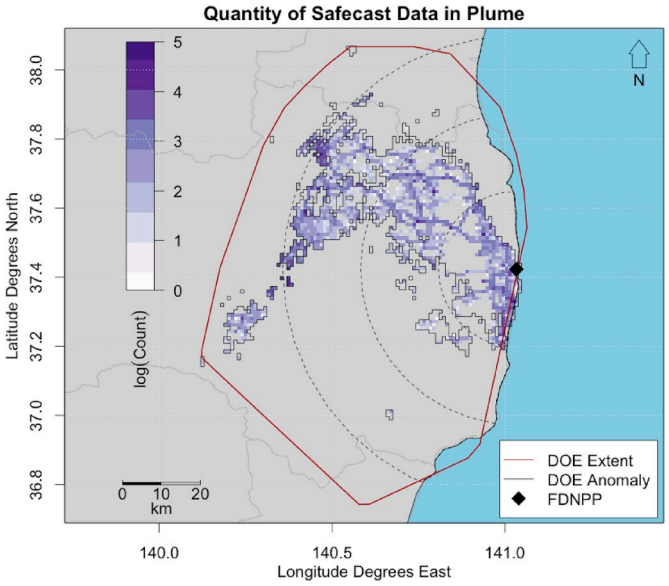

Fig. 4. Safecast devices collected millions of radiation measurements in the Fukushima area. Only Safecast data from within the DOE Anomaly outline is shown; that is, the plume region identified in the DOE data as having elevated radiation levels.

DOE and Safecast data for this paper are spatially standardized to half-kilometer areas and temporally standardized by decay correcting the data to the same time, the end of December 2016.

This work focuses on the most elevated area of radiation levels in order to identify if there is consistency in the models and datasets across the plume. Fig. 5 shows the spatial distribution of Gaussian, HYSPLIT, DOE, and Safecast as rasters in log(μSv/h). The modelled distributions of elevated radiation levels overlap with the high concentrations of ^{137}Cs for the plume visible on land in the DOE and Safecast datasets. In Fig. 5, the distribution of high values in the plume are similar in the models and observed data that were decay corrected to December 2016 in order to use more of the contributed measurements. The source of the release is indicated along the coastline by a diamond to show the location of the FDNPP.

The models and data are spatially visualized and the values are compared using histograms in Fig. 5. In this way, we compare variations of the model to observed values. Then the model and data are further spatially compared with each other by examining the distribution using cross-sections. Cross-sections are typically used as a method to compare models as the values might be accurate in general, but the trends may be distributed differently across the plume.

The Gaussian and HYSPLIT models simulate the dispersion of radiation continuously over space. The Gaussian model is limited by only dispersing in one direction, while the HYSPLIT model indicates a turn from a northwest direction to the southwest. However, the HYSPLIT model has a coarser resolution and does not account for large changes over short distances. The HYSPLIT model was downscaled for comparison and accurately simulates the variations from the central trajectory of the plume for the first 60 km which is the extent of the spatial coverage of the DOE dataset in the Fukushima area. The spatial extent of this study is limited to observational radiation data only over land. The comparable DOE government data thoroughly covers the Fukushima prefecture, but it is constrained to 60 km out from the point of release. The DOE and Safecast data confirm, with airborne and ground observations respectively, that there were elevated levels of radiation in this area. Safecast confirms elevated levels in the years since 2011, but the data are primarily in areas of human activity and the coverage is particularly sparse in areas of complex terrain (e.g. mountains, water features) and highly elevated levels of radiation.

Cross-sections were selected across the plume of elevated radiation levels, as seen in Fig. 6, with a focus on areas that have coverage from multiple sources. The location of the damaged nuclear power plant is indicated by the diamond along the coast and dashed black lines are used to indicate distances of 20, 40, and 60 km from the source. The red lines numbered from L1 to L9 are the locations of values taken for the cross-sections shown in the following plots.

In the cross-section plots, Figs. 7 and 8, the data follow similar trends at distances from the FDNPP. The distributions of values match well in areas of overlap; cross-section Lines 1 and 2 show a consistent match between the Gaussian model and the datasets. However, while HYSPLIT, shown as a blue line in the graphs, peaks at a consistent section across the plume at Lines 1 and 2, it also extends to high values in an area to the southwest that is not strongly indicated by the other three sources.

The plots of Fig. 7 bring awareness to the spatial properties of each of the models and datasets as not every area has coverage by all the sources. The Gaussian model is narrow at the start, as seen as the red graph line for the cross-section Line 1, but peaks in the same areas as both of the datasets. This model does not cover all the elevated areas of radiation, such as seen for cross-section Line 8, which is away from the central direction of the plume. The values from the HYSPLIT model, displayed as a blue line in the graphs, are elevated at most of data confirmed places, but the model does not peak there. HYSPLIT does not have a fine spatial resolution to pick up local variability such as large changes of values over small distances and it shows broad elevated areas further to the southwest than the other sources. The Safecast data, with values displayed as a green line, is consistent with the DOE data with values displayed as a black line. However, the contributed data are not always present in the highest areas, as seen in cross-section Lines 2 and 3, where the Safecast data peaks consistently, but there is not full coverage so the line of Safecast values stops from a lack of data right at or before the peak. Therefore, the Safecast data are able to identify an area with elevated levels of radiation, but in this case, it is not clear if it is the peak maximum value as the spatial coverage in this elevated part is limited.

Fig. 8 shows the values extracted from along a central line of the plume. That is, Line 9 as seen in Fig. 6, which starts at the highest intensity of released radiation at the FDNPP (as indicated by the diamond along the coast) and extends northwest for 60 km. When extending lengthwise from the plume, all the models start at relatively high values near the damaged reactor and decrease as dispersing away

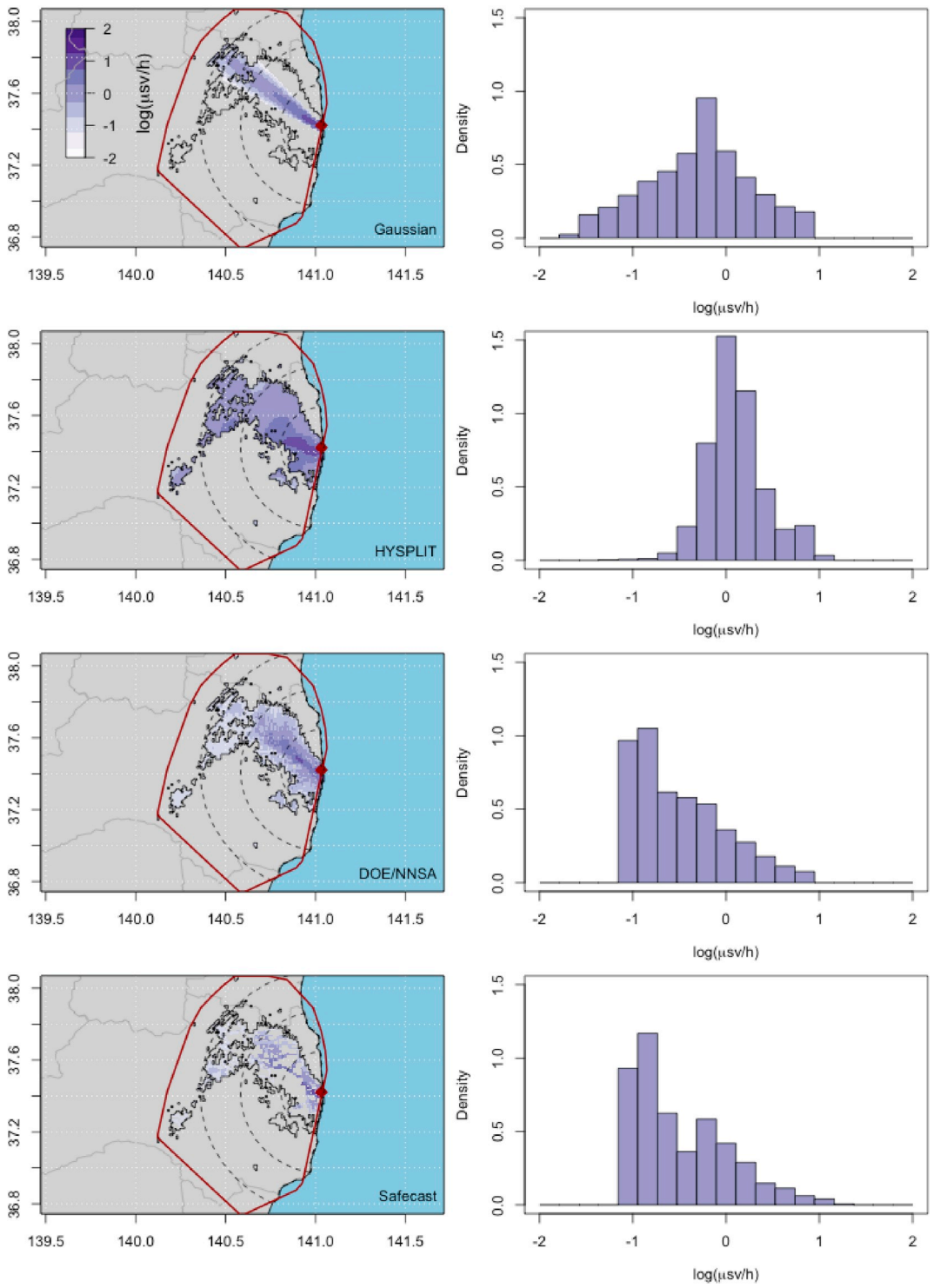

Fig. 5. Comparison of maps and histograms of values from the Gaussian model, HYSPLIT model, DOE data, and Safecast data.

to 60 km at which point the values are almost at natural background radiation levels. The Gaussian model peaks at a different place than all the other sources near the release location in an area that is actually indicated as a relatively lower section in all the other sources. The HYSPLIT model is very consistent with the datasets nearest the reactor for two peaks and two decreases. This model shows elevated levels about 30 km out at the same location, but it indicates values only half as high as the datasets at that location. Both of the models trail off to background levels at a slightly higher level than indicated by the datasets at 60 km. The DOE and Safecast data have consistent trends throughout, although, the Safecast data shows a 3μSv/h higher elevated level than DOE immediately near the reactor which is consistent with the HYSPLIT model. This peak, observed only in Safecast and HYSPLIT, may be a result of intensified deposition due to terrain and rainfall during the time period of the wind blowing to the northwest. However, this elevated area might not have been picked up by the other sources as the DOE is not ground based and the Gaussian model does not consider environmental factors such as terrain or rainfall.

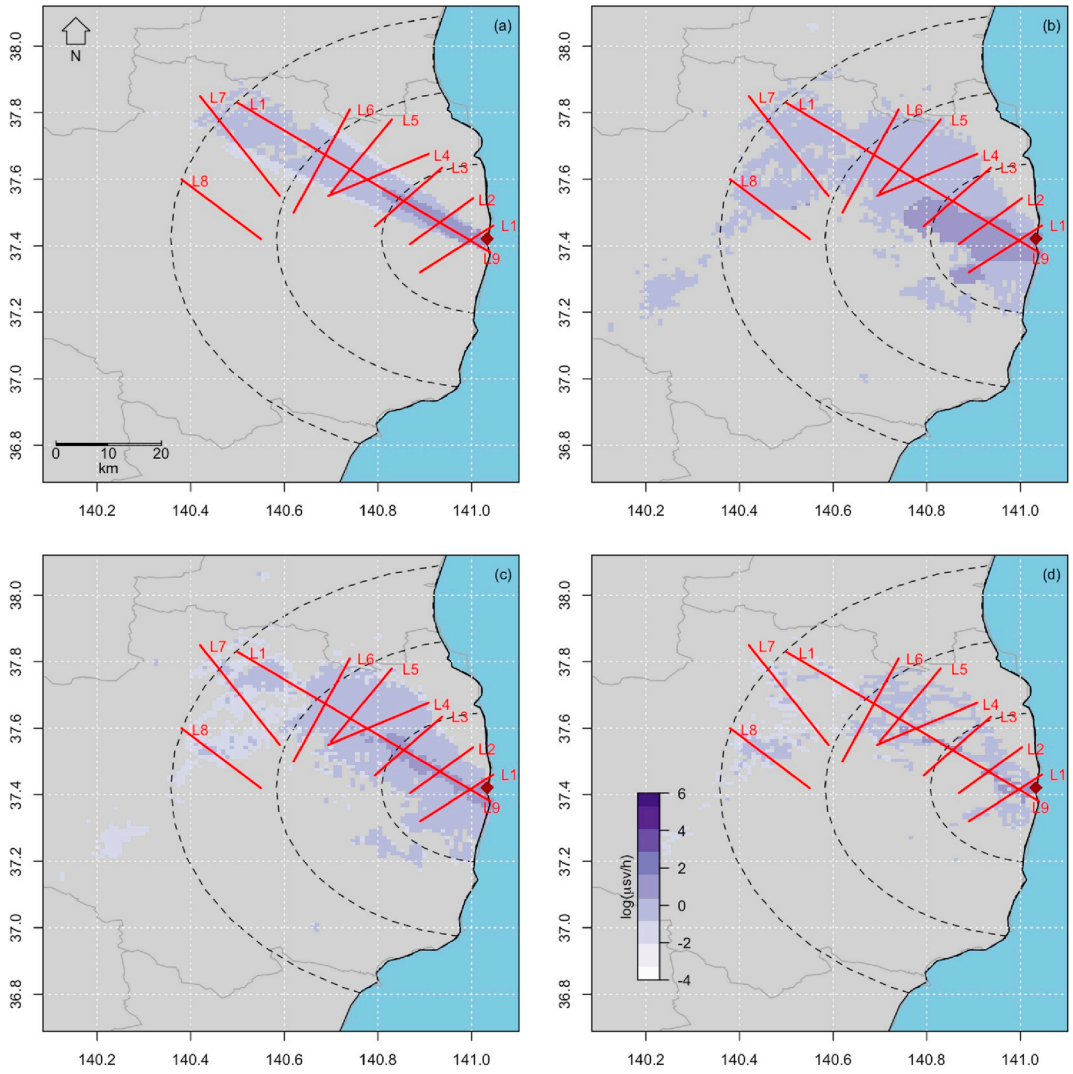

Fig. 6. Locations of cross-section lines across each of the models and datasets: (a) Gaussian, (b) HYSPLIT, (c) DOE, (d) Safecast.

5. Discussion

The atmospheric models and observational datasets show similar spatial variations for the elevated concentrations of radiation within the plume. A number of sampled cross-sections in areas of overlap gave insights into the spatial variations of the models when compared to observations from government and citizen science sources.

5.1. Models

The Gaussian model has a fine spatial resolution, but it is limited by dispersing consistently in one direction. This property can be acceptable over flat terrain, but the complex nature of terrain in Japan that changes dramatically within 60 km from the source leads to reliability issues as the mountains change the direction of dispersion. This model can be useful to get a quick result as it is not computationally intensive and it can be run at a fine spatial resolution. The Gaussian model did accurately indicate peaks, but it did not show all the areas that are elevated. The spatial limitations in the nature of the model should be understood when it is used and multiple models should be considered to best fit the properties of the location. Most importantly, the extent of this model indicating elevated levels should not limit the area that data are collected or serve as a boundary of the extent of elevated radiation levels.

The HYSPLIT model has a coarse resolution of 5 km compared to the data that was represented as a downscaled half-kilometer raster in this article. Significant changes over short distances can be better predicted in future modelling work by working with a finer resolution model; this is particularly useful in areas of elevated radiation concentrations. An even finer grid would be required to evaluate the greatest impacts which are near the reactor and, over a short distance, it might be more appropriate to use a model such as SCIPUFF instead. Although HYSPLIT can be run using a constant emission, instead of 3 h intervals, there are temporal limitations on meteorological data at a high spatial resolution. Although, it would cause a decrease in spatial resolution, the observational data could also be rasterized at a 5 km resolution surface in order to have a more direct comparison to the HYSPLIT model.

Dispersion models could be improved by representing complex environmental features that can impact the spatial distribution of the presence of elevated quantities of radioactive particles in the environment. Factors related to the absorption of ^{137}Cs radiation in the environment can be modelled with an implementation considering the high water solubility and the tendency of radionuclides to bind to clay which causes them to remain in the upper levels of the soil. Cesium follows potassium pathways and typically accumulates in soft tissues of plants. Primarily inactive tissue such as trunks of trees are rarely effected by radiation from the environment, but seeds can receive damage and debris fall again over the roots which recycles the radioactive nuclides. This cycle can make forested areas retain high levels of radioactivity. Plants receiving nutrients from the top layer of soil

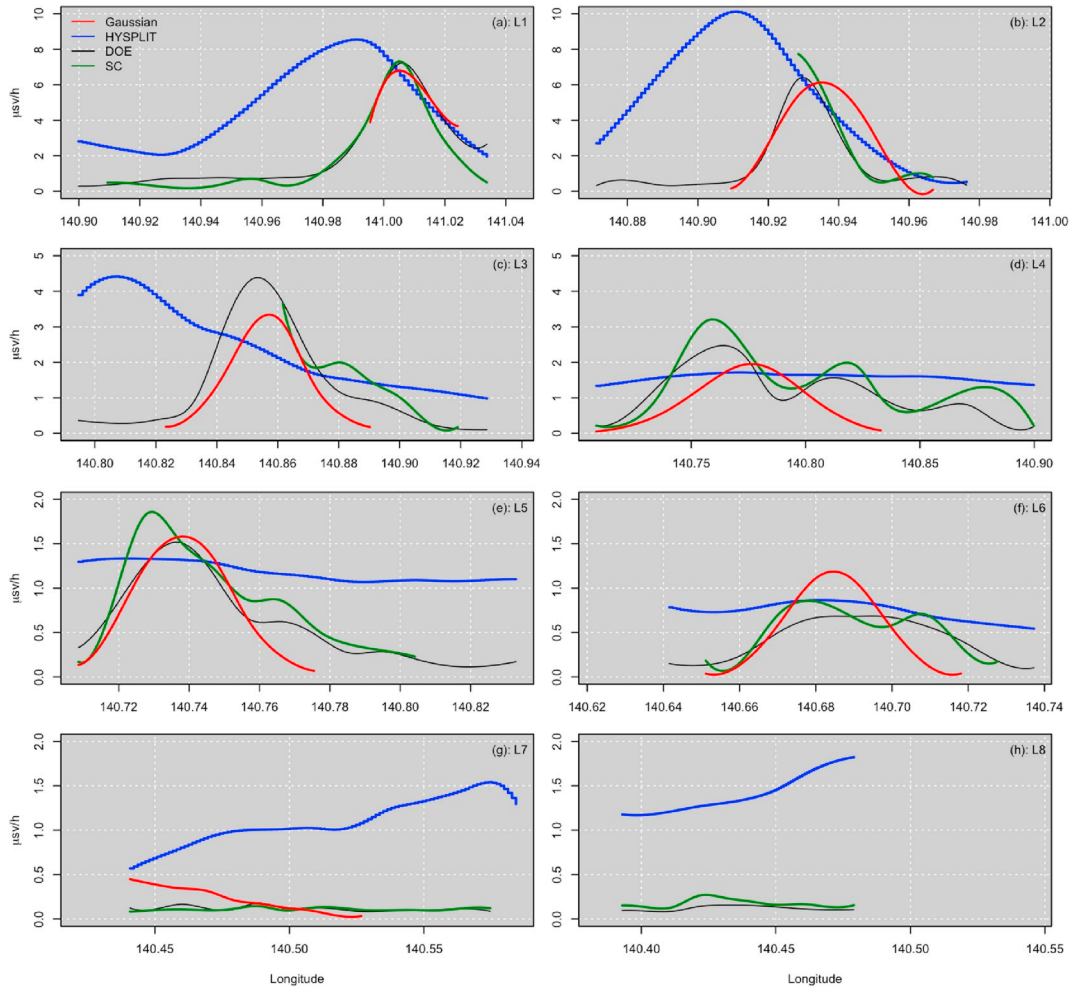

Fig. 7. Cross-section plots of eight lines across the plume as corresponding to the numbered lines in Fig. 6.

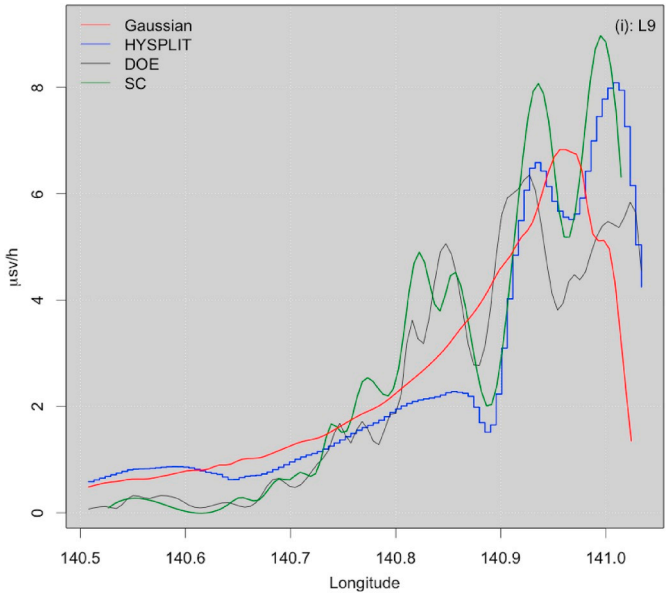

Fig. 8. Cross-section plot of line lengthwise along the plume as shown as L9 in Fig. 6.

typically have the highest radiation dosages such as found in grasses, mushrooms, and rice. These interactions can have associated environmental effects and could be modelled using land cover datasets to reflect the magnitude and extent of elevated radiation levels in the environment over many years.

5.2. Data

Additional ground truth observations can be used to improve the resolution of modelled distributions and to verify model outputs. This methodology is intended to improve models by identifying novel measurements that can be incorporated. Traditional sources of radiation data are produced by government agencies and industry. However, it is quite expensive to upkeep stations at a high resolution and the government network of sensors set up to provide measurements in Japan failed during the disaster (Nakamura and Kikuchi, 2011). While government agencies collected radiation measurements immediately after the event (Lyons and Colton, 2012), the data was not available to decision makers or the public immediately and the extent of the release was debated. The lack of sufficient coverage from static sensors made temporal shifts in intensity difficult to discern and the magnitude of the release from the source was not directly observed so source estimation is based on observations from the distribution.

Citizen science data could be incorporated into models in order to more accurately estimate areas lacking government data. While Safecast lacks the broad consistent spatial coverage as provided by airborne sensors, enough volunteered data are available on the ground to be able to interpolate in the plume of elevated levels and to decay correct data to future times. Some locations have thousands of measurements while traditional datasets often only have a few

measurements in the same spatial area. However, except for static sensors which provide limited coverage, there is no particular way of knowing if citizen science data will be collected in a certain area at a specific time. The uncertainty of coverage by volunteers can be mitigated by installing additional static sensors to provide spatio-temporal consistency or tasking collection in areas of interest. However, outside of the context of static sensors, there is a potential unintended risk of volunteers exposing themselves to elevated levels of radiation in order to collect measurements. This is contrary to the idea of volunteers simply carrying the device to understand environmental risk while going about their normal daily activities. The potential for behavior that could cause additional exposure is difficult to predict and the risk is situationally dependent, but the concept does spark ethical concerns which should be further evaluated.

6. Conclusions

This research presents a methodology for the comparison of observational data to model outputs of estimated non-steady release rate concentrations for the Fukushima radioactive release over land. Each model and dataset adds unique aspects of spatial and temporal resolution which gives insight into the actual spatial pattern of the phenomena when all the sources are standardized. HYSPLIT and Safecast identifying a peak of elevated levels near the reactor supports the case of the need to consider multiple sources and to not ignore limitations. Comparison of the atmospheric dispersion models with observational data confirms spatial variations of the release and the problem of relying on a single information source.

Government data are often difficult to access, not immediately made publicly available, and collection is costly to implement in a timely way for a long period of time. Citizen science environmental data has the capacity to meet environmental information needs, improve models, and impact decision making by contributing to situational awareness. The Safecast project serves a unique role by providing a long term source of radiation data in real-time at a high resolution in areas of human activity. The longitudinal nature of the citizen science data enabled comparison of multiple datasets by a method with validated decay correction. Citizen science is ideal for monitoring environmental levels in populated areas of interest, however, particularly in complex terrain and areas with extreme levels of radiation, there are limitations in the spatial resolution of the data. Instead of using the data by itself, it is most useful to integrate them with models and other datasets to reduce uncertainty by ensuring consistency in areas of overlap and confirming spatial patterns.

Concerns about environmental and human impacts can be addressed with validation of environmental data through on-the-ground monitoring that confirms the prediction of models representing dynamic behavior of radionuclides dispersed in the environment. This work focuses on areas of elevated radiation levels in order to identify if there is consistency in the models and datasets across elevated levels in the plume. Measurements are essential to improve performance and verify the distributions indicated by the models. In general, citizen science environmental monitoring can act as an early warning system and a rapid source of crisis information during disasters. Citizen science projects might become the main source of actionable data during future emergencies, including radioactive releases.

Acknowledgments

This research was funded by the Office for Naval Research (ONR) grant N00014-14-1-0208 and it was primarily conducted at the National Center for Atmospheric Research (NCAR). The authors gratefully acknowledge the NOAA Air Resources Laboratory (ARL) for the provision of the HYSPLIT transport and dispersion model and the READY website (http://www.ready.noaa.gov) used in this paper.

Appendix A. Supplementary data

Supplementary data to this article can be found online at https://doi.org/10.1016/j.atmosenv.2018.10.018.

References

Arya, S.P., 1999. Air pollution meteorology and dispersion. Oxford University Press, New York.
Bonner, S., Brown, A., Cheung, A., 2015. The Safecast Report. Tech. rep.. The Safecast Team.
Brown, A., Franken, P., Bonner, S., 2016. The Safecast Report. Tech. rep.. The Safecast Team.
Brown, A., Franken, P., Moross, J., Dolezal, N., Bonner, S., 2017. The Safecast Report. Tech. rep.. The Safecast Team.
Buytaert, W., Zulkafli, Z., Grainger, S., Acosta, L., Alemie, T.C., Bastiaensen, J., De BiÃvre, B., Bhusal, J., Clark, J., Dewulf, A., Foggin, M., Hannah, D.M., Hergarten, C., Isaeva, A., Karpouzoglou, T., Pandeya, B., Paudel, D., Sharma, K., Steenhuis, T., Tilahun, S., Van Hecken, G., Zhumanova, M., 2014. Citizen science in hydrology and water resources: opportunities for knowledge generation, ecosystem service management, and sustainable development. Front. Earth Sci. 2 (October), 1–21.
Cervone, G., Franzese, P., 2011. Non-darwinian evolution for the source detection of atmospheric releases. Atmos. Environ. 45 (26), 4497–4506.
Cervone, G., Franzese, P., 2014. Source Term Estimation for the 2011 Fukushima Nuclear Accident. Springer New York, New York, NY, pp. 49–64.
Cervone, G., Hultquist, C., 2018. Calibration of safecast dose rate measurements. J. Environ. Radioact. 190–191, 51–65.
Chai, T., Draxler, R., Stein, A., 2015. Source term estimation using air concentration measurements and a Lagrangian dispersion model - experiments with pseudo and real cesium-137 observations from the Fukushima nuclear accident. Atmos. Environ. 106, 241–251.
Coletti, M., Hultquist, C., Kennedy, W.G., Cervone, G., 2017. Validating safecast data by comparisons to a U. S. Department of Energy fukushima prefecture aerial survey. J. Environ. Radioact. 171, 9–20.
Connors, J.P., Lei, S., Kelly, M., 2012. Citizen science in the age of neogeography: utilizing volunteered geographic information for environmental monitoring. Ann. Assoc. Am. Geogr. 102 (6), 37–41.
Conrad, C.C., Hilchey, K.G., 2011. A review of citizen science and community-based environmental monitoring: issues and opportunities. Environ. Monit. Assess. 176 (1–4), 273–291.
Department of Energy, 2011. US DOE/NNSA Response to 2011 Fukushima Incident- Raw Aerial Data and Extracted Ground Exposure Rates and Cesium Deposition.
Diggle, P.J., Tawn, J.A., Moyeed, R.A., 1998. Model-based geostatistics. Appl. Stat. 47 (3), 299–350.
Draxler, R., Rolph, G., 2012. Modeling the Atmospheric Radionuclide Air Concentrations and Deposition from the Fukushima Daiichi NPP Accident. NOAA Air Resources Laboratory (ARL).
Du Bois, P.B., Laguionie, P., Boust, D., Korsakissok, I., Didier, D., Fiévet, B., 2012. Estimation of marine source-term following fukushima dai-ichi accident. J. Environ. Radioact. 114, 2–9.
Figueroa, P.M., 2013. Risk communication surrounding the Fukushima nuclear disaster: an anthropological approach. Asia Eur. J. 11 (1), 53–64.
Funabashi, Y., Kitazawa, K., 2012. Fukushima in review: a complex disaster, a disastrous response. Bull. At. Sci. 68 (2), 9–21.
Hanna, S.R., Tehranian, S., Carissimo, B., Macdonald, R.W., Lohner, R., 2002. Comparisons of model simulations with observations of mean flow and turbulence within simple obstacle arrays. Atmos. Environ. 36 (32), 5067–5079.
Hemmi, A., Graham, I., 2014. Hacker science versus closed science: building environmental monitoring infrastructure. Inf. Commun. Soc. 17 (7), 830.
Hengl, T., 2006. Finding the right pixel size. Comput. Geosci. 32 (9), 1283–1298.
Hultquist, C., Cervone, G., 2017. Citizen monitoring during hazards: validation of Fukushima radiation measurements. GeoJournal 83 (2), 189–206. https://doi.org/10.1007/s10708-017-9767-x.
Kinchy, A., Parks, S., Jalbert, K., 2016. Fractured knowledge: mapping the gaps in public and private water monitoring efforts in areas affected by shale gas development. Environ. Plann. C Govern. Pol. 34 (5), 879–899.
Korsakissok, I., Mathieu, A., Didier, D., 2013. Atmospheric dispersion and ground deposition induced by the Fukushima Nuclear Power Plant accident: a local-scale simulation and sensitivity study. Atmos. Environ. 70, 267–279. https://doi.org/10.1016/j.atmosenv.2013.01.002.
Lyons, C., Colton, D., 2012. Aerial measuring system in Japan. Health Phys. 102 (5), 509–515.
Matthias, V., Aulinger, A., Bieser, J., Cuesta, J., Geyer, B., Langmann, B., Serikov, I., Mattis, I., Minikin, A., Mona, L., Quante, M., Schumann, U., Weinzierl, B., 2012. The ash dispersion over Europe during the Eyjafjallajökull eruption - comparison of CMAQ simulations to remote sensing and air-borne in-situ observations. Atmos. Environ. 48, 184–194. https://doi.org/10.1016/j.atmosenv.2011.06.077.
McCormick, S., 2012. After the cap: risk assessment, citizen science and disaster recovery. Ecol. Soc. 17 (4), 31.
McGrath, M.J., Scanaill, C.N., 2013. Sensor technologies: healthcare, wellness, and environmental applications. Sens. Tech.: Healthc. Wellness Environ. Appl. 1–302.
Misawa, M., Nagamori, F., 2008. System for prediction of environmental emergency dose information network system. Fujitsu Sci. Tech. J. 44 (4), 377–388.
Nakamura, A., Kikuchi, M., 2008. What we know, and what we have not yet learned:

triple disasters and the fukushima nuclear fiasco in Japan. Publ. Adm. Rev. 893–899.
Nakamura, A., Kikuchi, M., 2011. What we know, and what we have not yet learned: triple disasters and the fukushima nuclear fiasco in Japan. Publ. Adm. Rev. 893–899.
Ottinger, G., 2010. Buckets of resistance: standards and the effectiveness of citizen science. Sci. Technol. Hum. Val. 35 (2), 244–270.
Povinec, P.P., Hirose, K., Aoyama, M., 2013a. Estimation of radiation doses. In: Radioactivity Impact on the Environment, pp. 325–360.
Povinec, P.P., Hirose, K., Aoyama, M., 2013b. Fukushima accident. In: Radioactivity Impact on the Environment, pp. 55–102.
Schade, S., Díaz, L., Ostermann, F., Spinsanti, L., Luraschi, G., Cox, S., Nuñez, M., Longueville, B.D., 2013. Citizen-based sensing of crisis events: sensor web enablement for volunteered geographic information. Int. J. Appl. Geomath. 5, 3–18.
Seymour, V., Haklay, M.M., 2017. Exploring engagement characteristics and behaviours of environmental volunteers. Citiz. Sci. Theory Pract. 2 (1), 1–13.
Srinivasan, T.N., Rethinaraj, T.S.G., 2013. Fukushima and thereafter : reassessment of risks of nuclear power. Energy Pol. 52, 726–736.
Stepenuck, K.F., Green, L.T., 2015. Individual-and community-level impacts of volunteer environmental monitoring: a synthesis of peer-reviewed literature. Ecol. Soc. 20 (3).
Sugiyama, G., Nassstrom, J., Foster, K., Pobanz, B., Vogt, P., Aluzzi, F., Homann, S., 2012. National atmospheric release advisory center dispersion modeling during the fukushima Daiichi nuclear power plant accident. In: NIRS Symposium on Reconstruction of Early Internal Dose Due to the TEPCO Fukushima Daiichi Nuclear Power Station Accident. Lawrence Livermore National Laboratory.
Terada, H., Katata, G., Chino, M., Nagai, H., Oct, 2012. Atmospheric discharge and dispersion of radionuclides during the Fukushima Dai-ichi Nuclear Power Plant accident. Part II: verification of the source term and analysis of regional-scale atmospheric dispersion. J. Environ. Radioact. 112, 141–154.
Tobler, W., 1987. Measuring spatial resolution. In: Proceedings of International Workshop on Geographic Information System.
Tomaszewski, B., MacEachren, a. M., 2012. Geovisual analytics to support crisis management: information foraging for geo-historical context. Inf. Visual. 11 (4), 339–359.
van der Velde, T., Milton, D.A., Lawson, T.J., Wilcox, C., Lansdell, M., Davis, G., Perkins, G., Hardesty, B.D., 2017. Comparison of marine debris data collected by researchers and citizen scientists: is citizen science data worth the effort? Biol. Conserv. 208, 127–138. https://doi.org/10.1016/j.biocon.2016.05.025.